

LASER COOLING

PACS numbers: 38.80.Pj
DOI: 10.1070/QE2006v036n03ABEH013132

Pulsed filling of a dark magnetooptical trap for rubidium atoms

P.L. Chapovsky

***Abstract*. The parameters of a dark magnetooptical trap for rubidium atoms are measured. The rubidium atoms captured and cooled in the trap occupy a hyperfine level of the ground electronic state, which does not interact with cooling laser radiation. The pulsed filling of the trap is produced due to desorption of rubidium caused by irradiation by a short (1 ms) light pulse. The trap captures and cools 2.5×10^8 rubidium atoms approximately for 0.2 s. The absorption spectra of a weak probe field by cold atoms are obtained, which demonstrate a good spectral resolution of the hyperfine structure in the excited state. This structure is completely hidden by the Doppler broadening in rubidium vapours at room temperature.**

Keywords: *laser cooling of rubidium, dark magnetooptical traps.*

1. Introduction

Magnetooptical traps (MOTs) have become the main tool for studying neutral atoms at ultralow temperatures ($T = 10^{-4} - 10^{-6}$ K) [1 – 5]. They contributed to the development of new fields in modern atomic physics such as the Bose – Einstein condensation of rarefied gases and laser spectroscopy of cold atoms, favoured the study of atomic collisions at ultralow temperatures, and stimulated many other investigations.

MOTs of early designs were filled by beams of slow atoms. However, simpler traps, in which atoms are captured and cooled directly from the surrounding gas of thermal atoms, have become most widespread [6]. Below, we will consider namely such systems.

The capture rate R of atoms in a MOT is proportional to the concentration n_a of thermal atoms in a vacuum chamber: $R \propto n_a$. The lifetime τ of trapped atoms is determined by a number of factors. First of all, the loss of an atom can be caused by its collisions with atoms of a residual gas in the vacuum system or with thermal atoms of a gas being cooled. The losses of atoms can also occur due to rather complicated processes of the electronic energy conversion to the translational motion of atoms [7]. In the simplest situation, when the losses of trapped atoms are caused only by collisions with thermal atoms of a gas being cooled, the lifetime of atoms in a trap is described by the relation $\tau \propto n_a^{-1}$, and the stationary amount $\overline{N}$ of trapped atoms proves to be independent on the concentration of thermal atoms [6]. Many applications of MOTs require long lifetimes of atoms in traps. However, an increase in the lifetime of atoms achieved by reducing the concentration of thermal atoms quite rapidly violates the situation at which $\tau \propto n_a^{-1}$, and the number of trapped atoms rapidly decreases.

There exist two methods to overcome this contradiction. In the first case, a MOT with two chambers is used. In the first chamber used for accumulation of atoms, the concentration of atoms being cooled is high, while in the second chamber used for confinement of trapped atoms, the concentrations of atoms is low. In the second case, a pulsed source of thermal atoms is used. This allows one to produce a high concentration of thermal atoms in the system only at the stage of trap filling and their low concentration at the stage of confinement of atoms in the trap. At present several schemes are proposed for pulsed filling of MOTs.

In [8, 9], standard getters of rubidium were used in the pulsed heating regime for pulsed filling of MOTs. The authors of [9] have demonstrated by this method a comparatively rapid (approximately for 3 s) trapping of more than 10^8 atoms and their subsequent confinement in the trap for ~ 13 s. Note that the accumulation time of atoms for a standard MOT with a stationary concentration of thermal atoms is equal to their lifetime in the trap. It seems that a substantial disadvantage of getters with pulsed heating is their large inertia.

A promising pulsed source of atoms can be based on photoinduced desorption, which is well known for alkali metal atoms (see [10] and references therein). This effect was used for laser cooling of atoms in papers [10, 11]. The authors of [10] performed the photoinduced desorption of Rb from the inner surface of the trap chamber made of stainless steel by the light from a halogen lamp producing the illumination of ~ 10 W cm^{-2}. In [10], $\sim 1.3 \times 10^8$ rubidium atoms were captured in the trap for the characteristic time 67 s. Without the photoinduced desorption of rubidium, the trap captured only $\sim 2 \times 10^7$ atoms for a much longer time of ~ 500 s. By using the photoinduced desorption of rubidium to fill the trap, the authors of [10] combined in one vacuum system the accumulation of atoms in the MOT and the subsequent Bose – Einstein condensation of atoms in the trap.

P.L. Chapovsky Institute of Automation and Electrometry, Siberian Branch, Russian Academy of Sciences, prosp. akad. Koptyuga 1, 630090 Novosibirsk, Russia; e-mail: chapovsky@iae.nsk.su

Received 7 October 2005
Kvantovaya Elektronika **36** (3) 257 – 262 (2006)
Translated by M.N. Sapozhnikov

In [11], desorption of rubidium atoms from a glass surface coated with polydemethylsiloxane film was performed by light from a photographic flashlamp. The authors have demonstrated a very rapid (for 65 ms) trapping of a great number (2.5×10^7) of rubidium atoms.

In [12], a special design of traps for alkali metal atoms was proposed, which provides the accumulation of atoms in the central part of the trap on a hyperfine level of the ground electronic state, which does not interact with the cooling field (the 'dark state'). As in [13], we will call such systems dark magnetooptical traps (DMOTs). Such traps are used to obtain the Bose–Einstein condensation of atoms. They also offer the unique possibilities for spectroscopic studies of the clouds of cold atoms that are not disturbed by strong laser fields forming the magnetooptical trap.

The pulsed filling of a DMOT has an additional important advantage. The matter is that the repumping laser radiation should be present at the DMOT periphery and absent at its central part. The formation of the dark region at the trap centre is prevented by the resonance scattering of repumping radiation by thermal atoms in a gas. The pulsed filling of the trap should reduce the scattering of repumping laser radiation by thermal atoms at the confinement stage of atoms in the trap.

The aim of this paper is to study the parameters of a DMOT for rubidium atoms filled in the pulsed regime by using the photoinduced desorption of Rb from the internal surface of a glass vacuum chamber.

2. Rubidium levels and a dark magnetooptical trap

The operation principle of a DMOT can be simply explained by considering the operation of a standard trap for rubidium atoms. The energy level diagram of rubidium atoms ^{85}Rb is presented in Fig. 1. The 780.2-nm D_2 absorption line of rubidium is used for trapping and cooling. A MOT is formed by six laser beams at the frequency shifted to the red from the centre of the $F_g = 3 \rightarrow F_e = 4$ transition. Due to the Doppler effect, the radiation at such detuned frequency interacts mainly with counterpropagating atoms. The momentum repumping from radiation to the atoms produces a dissipative radiative force directed toward their movement, thereby resulting in their cooling. To produce the spatial dependence of the light pressure force, circularly polarised radiation is used, and atoms are placed into a quadrupole magnetic field linearly increasing from the trap centre.

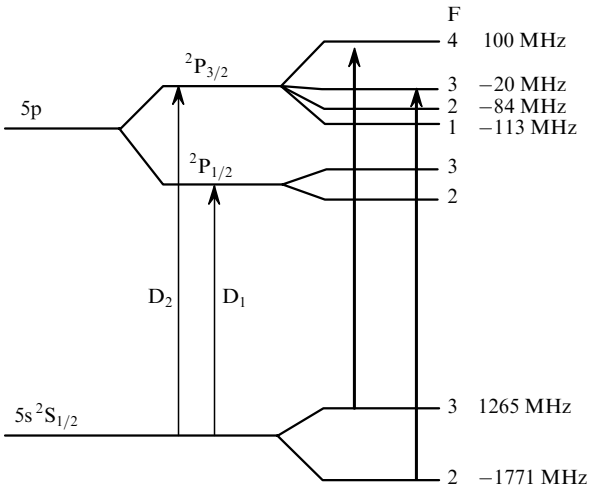

Figure 1. Scheme of the fine and hyperfine level splittings of ^{85}Rb. The frequencies indicate the hyperfine level shifts [17].

The $F_g = 3 \rightarrow F_e = 4$ transition in ^{85}Rb is *a cyclic transition* in the sense that the atom in the upper state cannot undergo the transition to the $F_g = 2$ hyperfine level of the ground state and is repeatedly involved in absorption. However, excitation into the wing of the $F_g = 3 \rightarrow F_e = 3, 2$ absorption line causes nevertheless the transition of the atom to the $F_g = 2$ state, thereby removing it from the cooling process even before trapping. To return the atom to the $F_g = 3$ level, the repumping radiation from an additional laser, which is resonant with the $F_g = 2 \rightarrow F_e = 2, 3$ transitions, is used.

The minimal temperature of atoms in the MOT can approach the so-called Doppler limit T_D [5], which is determined by the balance of cooling the atoms upon absorption of laser radiation and their heating due to recoil upon spontaneous emission. For rubidium atoms, the Doppler limit is $T_D \simeq 140$ μK.

A simple model of the MOT is based on the concept of the critical velocity v_c [6]. Atoms having the velocity $v < v_c$ are slowed down during their flight through the intersection region of laser beams so that they are captured in the trap. The flux of atoms with $v < v_c \ll v_0$ inside the unit spherical surface is $j = n_a v_0 \pi^{-1/2} 4^{-1} (v_c/v_0)^4$, where v_0 is the most probable velocity of the Maxwell distribution of atoms. The total capture rate of atoms is $R = jS$, where S is the area of the trap surface. The balance of the number N of particles in the trap is described by the differential equation [7]

$$\frac{dN}{dt} = R - N(\gamma_{Rb} + \gamma_b) - \beta \int n^2 d^3 r, \qquad (1)$$

where γ_{Rb} and γ_b are the frequencies of collisions knocking out cold atoms from the trap with thermal Rb atoms and particles of residual gases, respectively; and β is the factor determining the losses of atoms due to the conversion of the electronic excitation to the translational motion. Among many processes determining the lifetime of atoms in the trap, the most important are collisions of cold atoms with surrounding thermal Rb atoms (in our case) and particles of residual gases. By estimating the role of such collisions, one should bear in mind that the cross sections for collisions knocking out the atoms from the trap are far higher than gas-kinetic cross sections because, to knock out an atom from the trap upon a collision, it is sufficient to impart to it the velocity exceeding only v_c.

The production of atoms at a high density in the trap is prevented by their mutual repulsion during radiation repumping between them (see, for example, [14]). This process is rather complicated in the quantum limit, when the recoil energy of the atom $\hbar\omega_r = \hbar^2 k^2/2m$ becomes comparable with the energy $\hbar\omega_{vib}$ of the vibrational quantum in the trap. If $\omega_r \gg \omega_{vib}$, the exchange by photons can be estimated by neglecting the quantisation of the spatial movement of atoms. The resonance absorption cross section for photons in this case is $\sim\lambda^2$ [14].

The repumping radiation in a DMOT has the dark area at the trap centre. As a result, the atoms are trapped and

cooled at the trap periphery. At the central region, the atoms populate the $F_g = 2$ hyperfine level due to hyperfine pumping and do not interact with the strong field of a cooling laser. This results in two important consequences. First, the losses of atoms due to conversion of their electronic excitation to the translational motion are reduced. Second, the repulsion of atoms due to resonance radiation trapping is decreased. The main disadvantage of the DMOT is the reduction of the critical velocity v_c caused by the fact that a part of the cooling radiation energy is not used.

The DMOT quality is determined by the degree of suppression of the repumping laser radiation at the trap centre. A complete suppression cannot be achieved because scattering from optical elements is always present, and radiation is also scattered by thermal atoms of a gas being cooled. As a result, the limiting atomic concentrations in DMOTs are determined by the same physical processes as in common MOTs, but with considerably weaker light pressure forces and at considerably higher concentrations of trapped atoms [12].

3. Scheme of the setup

Our DMOT is a modification of the trap described in [15]. We use in the modified trap a higher-power laser providing ~ 6 mW in each of the six beams forming the trap. The diameters of these laser beams are increased up to ~ 1.5 cm. In addition, the system of repumping beams is modified and is now formed by two broad 5-mW beams of diameter ~ 1.5 cm having a dark field of diameter 5 mm at the centre. The repumping beams are directed to the trap centre at an angle of 90° to each other. Thus, repumping radiation is present at the trap periphery and is absent at its centre.

The basic components of the trap are shown in Fig. 2. The chamber is a glass flask of diameter 6 cm permanently connected to an ion pump through a glass tube of diameter 15 mm and length 25 cm. The pressure of residual gases in the chamber was kept at a level of 10^{-9} Torr. A glass appendix with metal rubidium was connected to the vacuum line at a distance of 5 cm from the trap centre. To reduce the Rb vapour pressure in the vacuum chamber of the trap, the appendix was cooled with a Peltier element down to $\sim 5\,^{\circ}$C.

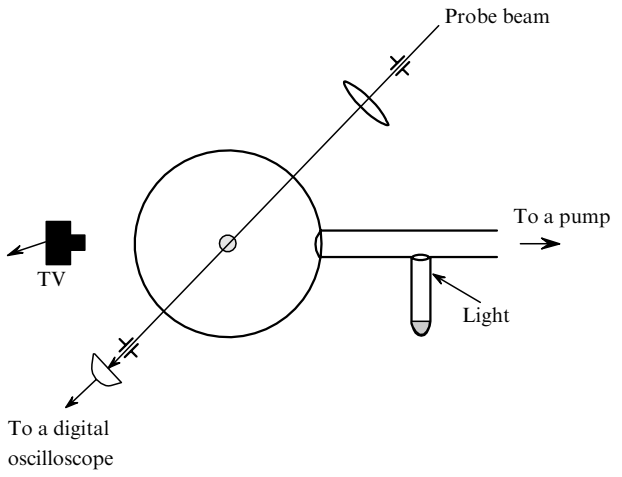

Figure 2. Scheme of measuring the DMOT parameters. Cooling and repumping beams, and Helmholtz coils are not shown. The appendix with Rb is cooled by a Peltier element down to ~5 °C.

The probe beam for measuring the concentration of trapped atoms was produced by a 20-mW ML6XX24 Mitsubishi laser diode. The diode temperature was maintained at $\sim 14\,^{\circ}$C with the stability better than 1 mK with the help of a Peltier element equipped with a temperature controller. The laser was tuned by varying the laser current. The probe-beam power used in experiments was sufficiently low (less than 30 nW) to avoid the power saturation of absorption. To detect a low-power probe beam, a highly sensitive photodetector protected from fluorescence of thermal and cold atoms in the trap was required. We used a photodetector with a sensitivity of 7 V μW^{-1}, a time resolution of ~ 0.1 ms, and a dark noise of ~ 2 mW. To protect the detector from external illumination, the probe beam was restricted with a small 2-mm aperture and was focused by a lens with $f = 210$ mm on the second small aperture located at a distance of 40 mm from the trap centre. The probe-beam diameter in the trap was ~ 0.3 mm.

The spatial characteristics of the cloud were measured by fluorescence recorded with a video camera whose image was digitised and then processed mathematically. The probe beam was aligned to the cloud centre by observing a weak perturbation of the cloud fluorescence produced by the beam when its power was specially increased.

The pulsed desorption of Rb was produced by the light of a photographic flashlamp, which was directed through the glass wall of the vacuum system to a rubidium film placed inside the upper part of the appendix (Fig. 2). The light pulse duration was approximately 1 ms. The flashlamp trigger was used to start the scan of the probe-beam frequency after the desirable time delay.

4. Photodesorption of rubidium atoms

Rubidium atoms are desorbed in our system from the glass surface, on which no additional coatings were deposited, as was done, for example, in [11]. The concentration of thermal atoms in the MOT chamber was measured by the linear absorption of weak probe radiation. The measured absorption spectrum was compared with calculations, which can be easily performed because it is known that the excited-state lifetime of Rb is 25 ns [16] and the hyperfine splittings [17] and angular momenta of the hyperfine states (Fig. 1) are also known. The Doppler width of the transition line at room temperature is $kv_0 = 310$ MHz. The accuracy of measuring the Rb concentration by this method is $\sim 10\,\%$ (see details, for example, in [18]).

Figure 3a shows two absorption spectra of thermal rubidium atoms in the region of the D_2 line. Spectrum (*1*) was recorded before the light flash, and spectrum (*2*) – within 15 ms after the light flash. The quadrupole magnetic field of the trap was not switched on during these measurements, and hence, rubidium atoms were not trapped. One can see from spectrum (*1*) that no absorption lines are recorded in the absence of illumination by the flashlamp. As a result, taking the absorption length of 6 cm into account, we can estimate the concentration of thermal rubidium atoms as $n_{Rb} \lesssim 1 \times 10^8$ cm^{-3} (the total concentration of rubidium of the natural isotopic composition). This value is considerably lower than the concentration of saturated rubidium vapours at a temperature of 5 °C (the appendix

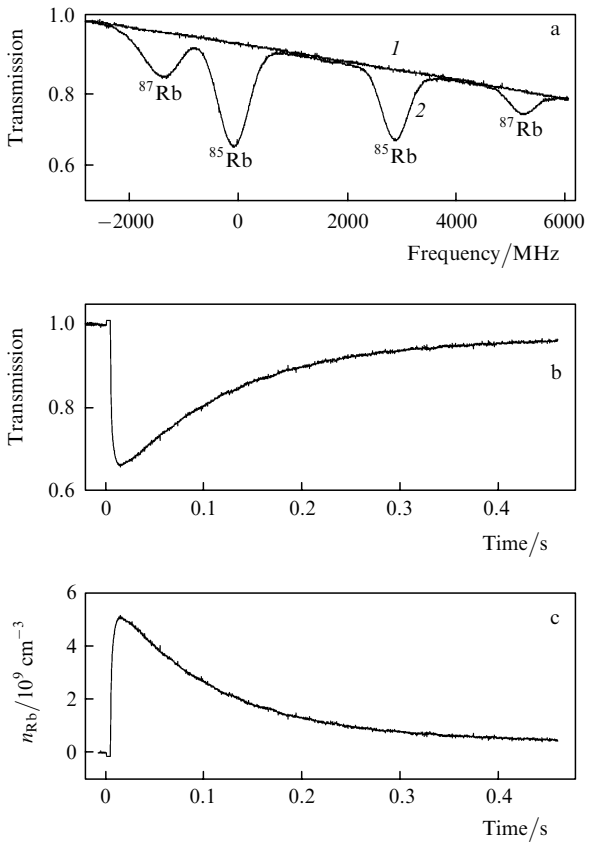

Figure 3. Results of measuring the concentration of desorbed rubidium atoms: the transmission spectrum in the stationary regime (*1*) and within $\sim$ 15 ms after the light flash (*2*) (a); the time dependence of transmission at the centre of the $F_g = 3 \rightarrow F_e$ line of the ^{85}Rb isotope (b); and the concentration dynamics of thermal Rb atoms in the DMOT chamber (c).

temperature), which is equal to 4×10^8 cm^{-3} [19, 20], because of the permanent pumping out of rubidium vapour with an ion pump.

Photoinduced desorption allows a temporary increase in the concentration of thermal rubidium atoms in the system. Spectrum (*2*) recorded within 15 ms after the light flash (Fig. 3a) exhibits fours strong absorption lines corresponding to transitions from the hyperfine levels of the ground electronic state of two stable rubidium isotopes ^{87}Rb and ^{85}Rb. The hyperfine structure of the excited state is hidden by the Doppler line broadening and is not resolved in this spectrum.

Figure 3b presents the absorption dynamics at the centre of the $F_g = 3 \rightarrow F_e$ transition of the ^{85}Rb isotope. The contribution to the photodiode signal from the flashlamp is suppressed and is observed only as a small positive rectangular pulse before the onset of the absorption signal. Figure 3c shows the concentration dynamics of thermal rubidium atoms calculated from the data in Fig. 3b.

The concentration of thermal rubidium atoms increases up to its maximum value equal to 5×10^9 cm^{-3} for $\sim$10 ms, while the characteristic lifetime of desorbed atoms in the MOT chamber is 150 ms. Note also that the desorbed atoms relax approximately exponentially during the first 200 ms and then slower at longer times.

5. Pulsed filling of the trap

5.1 Cloud shape

The suppression of the repumping radiation at the trap centre is not complete due to the scattering of repumping radiation by vacuum-chamber walls and rubidium atoms outside the dark region. A weak residual repumping radiation at the central region of the trap causes the resonance fluorescence of trapped atoms in the field of strong cooling radiation. The fluorescence intensity of atoms captured in the DMOT is considerably weaker than fluorescence of atoms in a standard trap. The light pressure force of the cooling field in the DMOT is also substantially weaker than that in a standard trap, and the cloud of cold atoms has the shape of a regular ellipsoid of revolution. The cloud shape differs from spherical because the magnetic-field gradient along the symmetry axis of Helmholtz coils is twice that in the transverse direction.

Figure 4 shows the cloud images in the stationary regime and upon pulsed desorption of rubidium atoms in the DMOT. The spatial distribution of fluorescence of atoms in the trap measured from these data is presented in Fig. 5. Before switching on the flashlamp, the width (FWHM) of the cloud in the plane perpendicular to the symmetry axis of the quadrupole magnetic field was 0.66 mm and along the symmetry axis – 0.5 mm. An increase in the concentration of thermal rubidium atoms in the DMOT chamber due to photodesorption of rubidium leads to a considerable increase in the amount of trapped atoms and the observed size of the cloud. Within 300 ms after the light flash, the FWHM of the cloud in the plane perpendicular to the symmetry axis of the quadrupole magnetic field was 1.5 mm and along the symmetry axis of the magnetic field – 1.1 mm. The emission intensity at the cloud centre increased by a factor of 2.6 compared to that in the stationary regime.

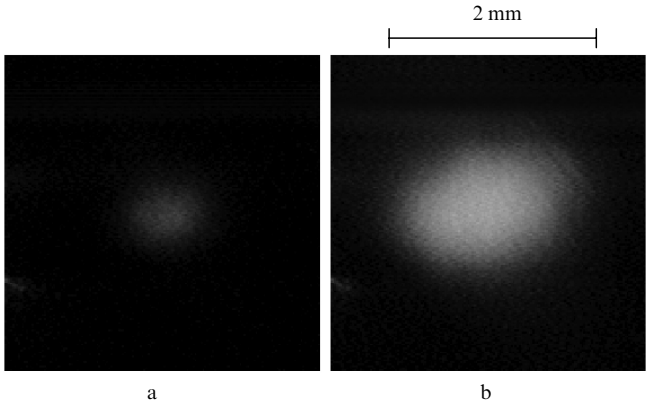

Figure 4. Fluorescence of the cloud of rubidium atoms in the DMOT before (a) and within 300 ms after (b) the light flash.

5.2 Absorption spectrum of cold atoms

The most reliable data on the amount of atoms captured in a DMOT can be obtained by measuring absorption of a weak probe radiation. Figure 6 [curve (*1*)] shows the transmission spectrum of a probe beam at the $F_g = 2 \rightarrow F_e = 1, 2, 3$ transitions by cold ^{85}Rb atoms in the trap in the stationary regime. The spectrum was recorded

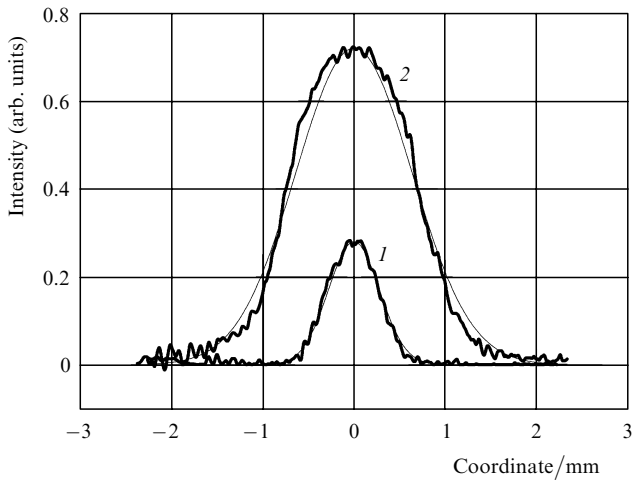

Figure 5. Spatial distribution of the fluorescence intensity of rubidium atoms in the trap in the plane perpendicular to the symmetry axis of the quadrupole magnetic field before (*1*) and within 300 ms after (*2*) the light flash. The thin curves are approximations by Gaussians.

during 10 ms, which was considerably longer than the time resolution 0.1 ms of a detector. Because the Doppler broadening of transitions was virtually absent in this case, the hyperfine splitting of the excited state was resolved. The approximation of this spectrum by the spectrum calculated for the concentration of cold atoms in the cloud $n_0 = 6.3 \times 10^{10}$ cm^{-3} is shown by the dashed curve in Fig. 6. One can see that the experimental intensities of the hyperfine $F_g = 2 \rightarrow F_e = 2, 3$ transitions are somewhat lower than the calculated ones. This is explained by a weak power saturation of the $F_g = 2 \rightarrow F_e = 2, 3$ transitions, which are saturated at a considerably lower radiation power than the cycling $F_g = 2 \rightarrow F_e = 1$ transition. The saturation intensity for the cycling $2 \rightarrow 1$ transition is ~ 5 mW cm^{-2}. The probe-beam intensity was two orders of magnitude lower. The transmission spectra were calculated assuming that the absorption lines

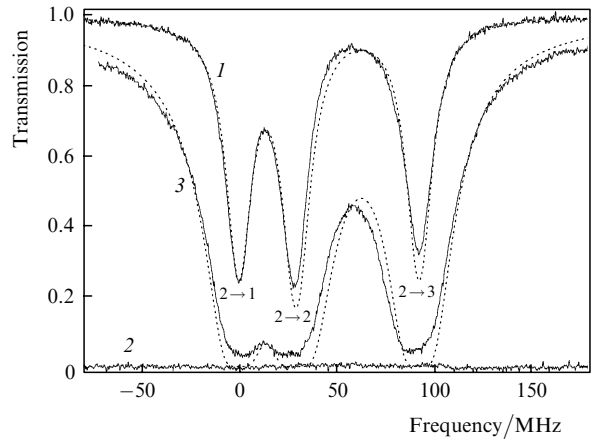

Figure 6. Absorption spectra of probe radiation by cold rubidium atoms in the DMOT at the hyperfine $F_g = 2 \rightarrow F_e = 1, 2, 3$ transitions in the ^{85}Rb isotope in the stationary regime (without Rb photodesorption) (*1*) and within 300 ms after the light flash (*3*). Curve (*2*) is the zero level (the probe beam is blocked and the flashlamp is switched on). The calculated spectra are shown by the dashed curve

had Lorentzian shapes with the homogeneous width (HWHM) of 5.6 MHz. Because the radiative width of the transition line was 3.1 MHz [16], the spectral width of the probe-beam radiation was ~ 2.5 MHz. By using the geometrical parameters of the cloud of cold atoms in the stationary regime presented above, we estimated the number of atoms captured in the stationary DMOT as $N_0 = 7.2 \times 10^6$.

The photodesorption of rubidium results in a considerable increase in the concentration of thermal atoms and especially in the amount of trapped atoms. In this case, the absorption of probe radiation becomes so strong that it is almost completely absorbed at the line centres. It was important to be sure in these measurements that scattered radiation does not displace the zero level of a detector of probe radiation. The detector zero level [curve (*2*) in Fig. 6] was recorded when the flashlamp was switched on and the probe beam was blocked. The absorption spectrum [curve (*3*)] was recorded within 300 ms after switching on the flashlamp. The transmission spectrum was calculated for the concentration of atoms in the cloud $n = 2 \times 10^{11}$ cm^{-3}. Taking into account the geometrical parameters of the cloud measured above, the total number of trapped atoms is $N = 2.5 \times 10^8$. Therefore, the photoinduced desorption of atoms in the DMOT allows the concentration of trapped rubidium atoms to be increased by a factor of $n/n_0 \simeq 3$ and the total number of trapped atoms by a factor of $N/N_0 \simeq 35$. These data concern the number of atoms at the $F_g = 2$ level of the ground state of ^{85}Rb. A smaller, but, however, noticeable number of atoms also occupy the $F_g = 3$ level.

The calculated transmission of the probe beam near the absorption line centre in the case of a great number of trapped atoms proves to be noticeably lower than the experimental value [curve (*3*) in Fig. 6]. The observed optical density at the $F_g = 2 \rightarrow F_e = 1$ transition line centre was 3.3, whereas the calculated optical density was 9.8. This can be explained by the following three reasons. First, the radiation of a semiconductor laser has the broadband component, which is not absorbed by rubidium atoms. Second, a part of the scattered probe radiation, which is always present in the optical system, is incident on the detector, by-passing rubidium atoms in the trap. Third, this can be caused by the comparable diameter of the probe beam and the size of the cloud of cold atoms and a higher transmission of radiation at the cloud periphery. We estimated the concentration of atoms in the cloud by absorption in the line wings, where the effect of all these factors is smaller.

We suppose that the apparent decrease in the optical density at the absorption line centre is mainly caused by the presence of the broadband component in the radiation of a semiconductor laser. We measured the transmission of radiation from a semiconductor laser in a strongly heated cell with rubidium vapours and found that at the absorption line centres a broadband background remained, as in experiments with cold atoms described above.

Figure 7 illustrates the trapping dynamics of atoms. The characteristic filling time of the trap was approximately 150 ms. Therefore, the capture rate is rather high (1.7×10^9 atom s^{-1}). This rate is only an order of magnitude smaller than the trap filling rate reported in [12], where a rather complicated Zeeman slower of sodium atoms and order-of-magnitude higher-power laser beams were used.

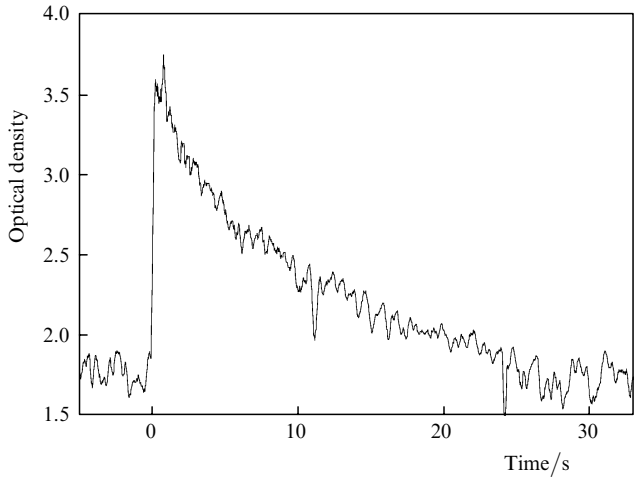

Figure 7. Time dependence of the optical density at the centre of the $F_g = 2 \rightarrow F_e = 1$ line of the ^{85}Rb isotope.

The characteristic confinement time of the cloud of cold atoms in our trap was ~ 10 s.

6. Conclusions

We have shown that the pulsed photodesorption of rubidium atoms is a convenient approach providing the combination of a low concentration of thermal atoms in a dark magnetooptical trap during the confinement of trapped atoms with a high concentration of thermal atoms during filling the trap. Pulsed photodesorption in the trap provided a temporary (for 150 ms) increase in the concentration of thermal rubidium atoms almost by two orders of magnitude, from 1×10^8 cm^{-3} to 5×10^9 cm^{-3}, which allowed a great amount of rubidium atoms to be trapped for 0.1–0.2 s. We have obtained the concentration of rubidium atoms in the dark magnetooptical trap equal to $n = 2 \times 10^{11}$ cm^{-3} and the total number of trapped atoms $N = 2.5 \times 10^8$, which is three and thirty-five times greater than the corresponding stationary values. The confinement time of atoms in the trap was ~ 10 s. The amounts of Rb atoms presented above concern the population of the hyperfine $F_g = 2$ level of the ground state of ^{85}Rb. In addition, a part of Rb atoms occupy the hyperfine $F_g = 3$ level. The population of this state was not measured in this paper.

The absorption spectra of Rb atoms in the dark magnetooptical trap with pulsed filling clearly demonstrate the convenience of this trapping method for spectroscopic investigations of cold atoms. These absorption spectra exhibit intense lines and are almost not affected by strong radiation fields forming the trap.

The stationary concentration of thermal rubidium atoms in our trap equal to 1×10^8 cm^{-3} corresponds to the pressure of rubidium vapours $\sim 3 \times 10^{-9}$ Torr. Such a pressure of the surrounding gas is still too high for a number of problems, for example, for obtaining the Bose–Einstein condensation of rubidium atoms [21]. However, we can hope that a deeper cooling of the appendix with metal rubidium than that used in this paper will allow us to reduce considerably the stationary pressure of rubidium vapours in the system, preserving nevertheless the possibility of a temporary production of rubidium at high concentrations by using photodesorpion for rapid and efficient filling the trap.

Acknowledgements. This work was supported by the Russian Foundation for Basic Research (Grant No. 03-02-17553) and the Presidium of the Siberian Branch, RAS (Grant 'Laser Cooling of Gases in Magnetooptical Traps').

References

1. Raab E.L., Prentiss M., Cable A., Chu S., Pritchard D.E. *Phys. Rev. Lett.*, **59**, 2631 (1987).
2. Chu S. *Rev. Mod. Phys.*, **70**, 685 (1998).
3. Cohen-Tannoudji C. *Rev. Mod. Phys.*, **70**, 707 (1998).
4. Phillips W.D. *Rev. Mod. Phys.*, **70**, 721 (1998).
5. Balykin V.I., Minogin V.G., Letokhov V.S. *Rep. Progr. Phys.*, **63**, 1429 (2000).
6. Monroe C., Swann W., Robinson H., Wieman C. *Phys. Rev. Lett.*, **65**, 1571 (1990).
7. Weiner J., Bagnato V.S., Zilio S., Jullenne P.S. *Rev. Mod. Phys.*, **71**, 1 (1999).
8. Fortagh J., Grossmann A., Hansch T.W., Zimmermann C. *J. Appl. Phys.*, **84**, 6499 (1998).
9. Rapol U.D., Wasan A., Natarajan V. *Phys. Rev. A*, **64**, 023402 (2001).
10. Anderson B.P., Kasevich M.A. *Phys. Rev. A*, **63**, 023404 (2001).
11. Atutov S.N., Calabrese R., et al. *Phys. Rev. A*, **67**, 053401 (2003).
12. Ketterle W., Davis K.B., Joffe M.A., Martin A., Pritchard D.E. *Phys. Rev. Lett.*, **70**, 2253 (1993).
13. Chu S. *Nature*, **416**, 206 (2002).
14. Castin Y., Cirac J.I., Lewenstein M. *Phys. Rev. Lett.*, **80**, 5305 (1998).
15. Chapovsky P.L. *Zh. Eksp. Teor. Fiz.*, **127**, 1035 (2005) [*J. Exp. Theor. Phys.*, **100**, 911 (2005)].
16. Schmieder R.W., Lurio A., Happer W., Khadjavi A. *Phys. Rev. A*, **2**, 1216 (1970).
17. Barwood G.P., Gill P., Rowley W.R.C. *Appl. Phys. B*, **53**, 142 (1991).
18. Permyakova O.I., Yakovlev A.V., Chapovsky P.L. *Kvantovaya Elektron.*, **35**, 449 (2005) [*Quantum Electron.*, **35**, 449 (2005)].
19. Nesmeyanov A.N. *Davlenie para khimicheskikh elementov* (Pressure of Vapours of Chemical Elements) (Moscow: Izd. Akad. Nauk SSSR, 1961).
20. Lide D.R. (Ed.) *CRC Handbook of Chemistry Physics* (Boca Raton, Fl, USA: CRC Press, 1993).
21. Cornell E.A., Wieman C.E. *Rev. Mod. Phys.*, **74**, 875 (2002).